Studies on Strain and Temperature Characteristics of a Slanted Multimode Fiber Bragg Grating and Its Application in Multiwavelength Fiber Raman Ring Laser

Chun-Liu Zhao, Zhaohui Li, M. S. Demokan, *Senior Member, IEEE*, Xiufeng Yang, Wei Jin, *Senior Member, IEEE*, and Chao Lu, *Member, IEEE*

Abstract—Detailed strain and temperature characteristics of a 2° slanted multimode fiber Bragg grating (MFBG) are developed theoretically and observed experimentally. Results show that the strain and temperature sensitivities are almost the same for different transmission dips of the 2° slanted MFBG. Utilizing two characteristics of the 2° slanted MFBG, namely 1) resonant wavelength intensities strongly affected by excited mode propagating before the grating and 2) uniform strain sensitivities of different resonant wavelengths, a switchable and tunable multiwavelength fiber Raman ring laser is realized. The configuration is simple and multipurpose. Results show that the laser can generate single-, dual-, three-, four-, and five-wavelength lasing by switching between each operation if a mode scrambler (MS) that is inserted in front of the slanted MFBG is adjusted; furthermore, a 4.2-nm continuous wavelength-tuning range is achieved by straining the slanted MFBG when the MS is fixed.

Index Terms—Fiber Raman laser, multiwavelength fiber laser, slanted multimode fiber Bragg gratings (MFBGs), wavelength switching, wavelength tuning.

I. INTRODUCTION

FIBER Bragg gratings (FBGs) have attracted much attention since the first demonstration by Meltz *et al.* [1] due to their wide applications in optical communications and optical fiber sensor systems. Optical fiber devices based on FBGs have been developed rapidly and used as spectral filters, dispersion compensators, gain-flattening filters, and sensors. To a lesser extent, multimode FBGs (MFBGs) have also received attention in recent years [2]–[9]. MFBGs show multiple reflection peaks in the reflection spectrum due to multimode coupling and are believed to have many potential applications in optical sensors, mode converters, and local area networks (LANs). Mizunami *et al.* [4] investigated the detailed spectral properties of FBGs in multimode fibers (MMFs), including temperature and polarization characteristics, theoretically and experimentally. Szkopek *et al.* [5] designed a novel MMF to fabricate narrow-band high-reflectivity FBGs. In optical sensor applications, Wanser *et al.* [2] and Mizunami *et al.* [6] proposed applications of MFBGs to bending sensors. Recently, MFBGs were also used in optical fiber lasers. In [7], a several-mode FBG was used as an element providing polarization hole burning in a dual-wavelength ytterbium-doped fiber laser. In addition, in [8], an MFBG was used as a tunable filter to realize a wavelength-switching erbium-doped fiber laser by using spatial-mode excitation and selection techniques. In [9], wavelength locking of a semiconductor laser was demonstrated by using an MFBG.

However, all MFBGs previously mentioned were simple uniform FBGs written by ultraviolet (UV) light into the core of MMFs. The different types of FBGs (i.e., uniform, apodized, chirped, and slanted) in single-mode fibers (SMFs) illustrate a wide variety of optical properties. Obviously, an understanding of the different types of MFBGs are important and basic for any possible applications of MFBGs. Slanted MFBGs show special and complex spectral properties because the slanted periodic perturbation in the fiber core causes coupling between various core modes and between cladding modes and radiation modes. Yang *et al.* [10] studied the effect of the grating slant in a graded-index MMF in what is believed to be the first paper dealing with MFBGs. In our recent paper [11], a 2° slanted MFBG was used as a comb filter in a switchable multiwavelength semiconductor optical amplifier (SOA) fiber ring laser. Experimental results showed that the stable five-wavelength lasing operation with a wavelength separation of ∼ 0.54 nm can be achieved at room temperature. However, detailed characteristics of a slanted MFBG have not been reported.

In this paper, we report detailed strain and temperature characteristics of a 2° slanted MFBG. Both the experimental and theoretical results show that the strain and temperature sensitivities are almost the same for different transmission dips of the 2° slanted MFBG. Furthermore, we apply the slanted MFBG to a fiber Raman ring laser to realize wavelength switching and continuous wavelength tuning. The 2° slanted MFBG can work
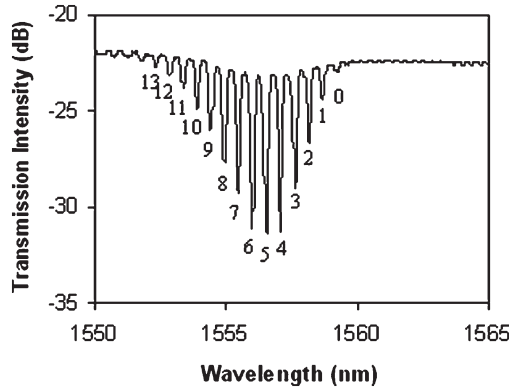
Fig. 1. Transmission spectrum of a 2° slanted MFBG.

as a switchable and tunable optical filter, utilizing two characteristics, namely 1) resonant wavelength intensities affected strongly by excited mode propagating before the grating and 2) uniform strain sensitivities of different resonant wavelengths. Our results show that the laser can generate single-, dual-, three-, four-, and five-wavelength lasing by switching between each operation if we adjust a mode scrambler (MS) that is inserted in front of the slanted MFBG; furthermore, a 4.2-nm continuous wavelength-tuning range is achieved by straining the slanted MFBG when the MS is fixed.

The remainder of this paper is constructed as follows: Section II describes the characteristics of a slanted MFBG. The wavelength variation of transmission dips arising from the strain and the temperature are predicted theoretically. Section III presents the experimental measurement of a 2° slanted MFBG. The measurements to determine strain and temperature dependence are described and compared with the analysis obtained from theory. Section IV describes the experimental demonstration of wavelength switching and tuning of a fiber Raman ring laser by using the 2° slanted MFBG. Section V contains the conclusion.

II. THEORY OF A SLANTED MFBG

Fig. 1 shows a typical transmission spectrum of a 2° slanted FBG in a graded-index MMF measured under the few-mode excitation condition. Because many modes can propagate simultaneously in the fiber core of an MMF, a slanted MFBG may couple light from some core modes to other backward-propagating core modes and/or cladding modes so that the transmission spectrum shows multitransmission dips. The MFBG thus behaves like a multireflection filter. The phase-matching condition or the Bragg reflection condition of the slanted MFBG can be expressed as [10]

$$\lambda = (n_i + n_j)\Lambda / \cos(\theta) \tag{1}$$

where λ is the reflected wavelength, Λ and θ are the index modulation period and the slanting angle of the MFBG, respectively, and n_i and n_j are the effective indexes of a forward-propagating core mode and a backward-propagating core (or cladding) mode. As mentioned in [10], the slanting angle θ of the MFBG will largely affect the properties of the grating. There are more transmission dips of a 2° slanted MFBG than

that of an MFBG without slant in the same few-mode excitation condition. Furthermore, θ will largely affect the kinds of couplings occurring in the grating, especially when θ is larger than 2°. In our experiment, the spectrum (Fig. 1) shows no change when we cover the surface of a 2° slanted MFBG with index-matching oil. This means that the couplings in the 2° slanted MFBG mainly occur between the core modes.

Because some of the core modes in a graded-index MMF have almost the same propagation constant (effective index), the modes having the same propagation constant are assumed to be the same principal mode [4], [5]. The effective index for the Nth principal core mode can be expressed as

$$n_N = n_{\rm co}\left[1 - \frac{\lambda\sqrt{2\Delta}}{\pi n_{\rm cl}a}(N+1)\right]^{1/2} \tag{2}$$

where $n_{\rm co}$ is the highest refractive index of the fiber core, $n_{\rm cl}$ is the refractive index of the fiber cladding, Δ is equal to $(n_{\rm co} - n_{\rm cl})/n_{\rm co}$, a is the radius of the core, and N is an integer.

When an axial strain is applied on the MFBG, transmission dips will shift to longer wavelengths because the Λ of the MFBG will increase with axial stretching. At the same time, the effective refractive index of every mode will increase due to the photoelastic effect of the fiber. Thus, from (1), the wavelength change of transmission dips arising from the strain can be written as [12]

$$\frac{\Delta\lambda}{\lambda} = \left\{\frac{n_i^3 + n_j^3}{2(n_i + n_j)}\left[(p_{11} + p_{12})\gamma - p_{12}\right] + 1\right\}\varepsilon \tag{3}$$

where p_{ij} is a component of the strain–optic tensor, γ is the Poisson's ratio, and ε is an axial strain applied to the MFBG. Meanwhile, the wavelength change caused by the temperature is given by [12]

$$\frac{\Delta\lambda}{\lambda} = \left\{\xi - \frac{n_i^3 + n_j^3}{2(n_i + n_j)}(p_{11} + 2p_{12})\alpha + \alpha\right\}\Delta T \tag{4}$$

where ξ is the thermooptic coefficient, α is the linear expansion coefficient, and ΔT is the temperature variation of the MFBG.

We define two parameters as follows: $K_\varepsilon = \Delta\lambda/\varepsilon$ is the strain sensitivity, and $K_T = \Delta\lambda/\Delta T$ is the temperature sensitivity. The K_ε and K_T of the transmission dip due to coupling between the ith and the jth principal core modes are related to the effective indexes of n_i and n_j, as shown in (3) and (4). Those two parameters for different transmission dips are different because the effective index is not the same for different principal core modes. However, the values of K_ε and K_T for different transmission dips are not different, as will be explained in Section III.

III. PROPERTIES OF A 2° SLANTED MFBG

In the experiment, a 2° slanted MFBG is fabricated in a hydrogen-loaded MMF using phase masks that are illuminated by UV light. The fiber is a standard graded-index MMF with a core diameter of 62.5 μm and a core refractive index of approximately 1.452. The phase mask has a constant period of
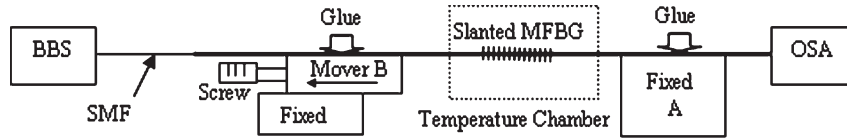
Fig. 2.   Measurement configuration for the slanted MFBG. Thin line: SMF. Thick line: MMF.

1073.6 nm so that the corresponding grating period is 536.8 nm. The exposure length is 12 mm. The spectrum measurements are performed using a broadband light-emitting diode (LED) source under the few-mode excitation condition where an SMF is spliced to an MMF. Thus, the light propagating in the MMF before reaching the grating will be mainly the zeroth principal mode. The transmission spectra are observed with an optical spectrum analyzer (Advantest Q8384) with a resolution of 0.02 nm.

Fig. 1 shows the transmission spectrum of the 2° slanted MFBG without strain at room temperature. The transmission wavelength range of the slanted MFBG is from 1551 to 1560 nm, and there are approximately 17 transmission dips with different losses. The dip with the longest wavelength (marked by the zeroth) is 1559.28 nm, and it is due to the coupling between the forward-propagating and the backward-propagating zeroth principal core mode. The dips marked from first to thirteenth are caused by the zeroth principal core mode coupling to the first up to the 13th principal core modes, respectively. The separation between these dips is approximately 0.54 nm, which is determined by the refractive index of the core and the cladding of the MMF. The wavelengths of dips in the middle (from the second to the ninth dips) are at 1558.17, 1557.63, 1557.10, 1556.56, 1556.02, 1555.48, 1554.95, and 1554.40 nm, respectively.

In the experiment, the strain dependence of the MFBG was studied by stretching the MFBG axially at room temperature, as shown in Fig. 2. The temperature dependence of the transmission spectrum was studied by placing the MFBG in a temperature chamber whose temperature is controlled in the range of 25–100 °C.

Fig. 3 shows the strain dependence of the slanted MFBG at room temperature. When the MFBG was gradually stretched by moving one translation stage precisely from 0 to 0.4 mm (which corresponds to 0–3500 $\mu\varepsilon$), the Bragg wavelengths shifted linearly to longer wavelength, but the strain sensitivities changed slightly. K_ε was approximately 1.2034, 1.2026, 1.2018, 1.2005, 1.1989, 1.1971, 1.1962, and 1.1956 pm/$\mu\varepsilon$ for different transmission dips (from the second to the ninth dips). K_ε becomes a little smaller with coupling to a higher order principal mode, but the difference between $K_{\varepsilon 2}$ and $K_{\varepsilon 9}$ was only approximately 7.8×10^{-6} nm/$\mu\varepsilon$. Fig. 4 shows the temperature dependence of the slanted MFBG without strain. When the temperature rose from 25 °C to 100 °C, the Bragg wavelengths also shifted linearly to longer wavelength. The temperature sensitivities of the eight marked (from the second to the ninth) transmission dips were $K_T = 13.831, 13.829, 13.825, 13.822, 13.819, 13.815, 13.811,$ and 13.806 pm/°C.

From (2)–(4), and using the material constants of the fiber ($p_{11} = 0.121, p_{12} = 0.27, \gamma = 0.17, \xi = 0.87 \times 10^{-5}$/°C, and $\alpha = 5.5 \times 10^{-7}$/°C [4], [12]), we expect the strain sensitivities
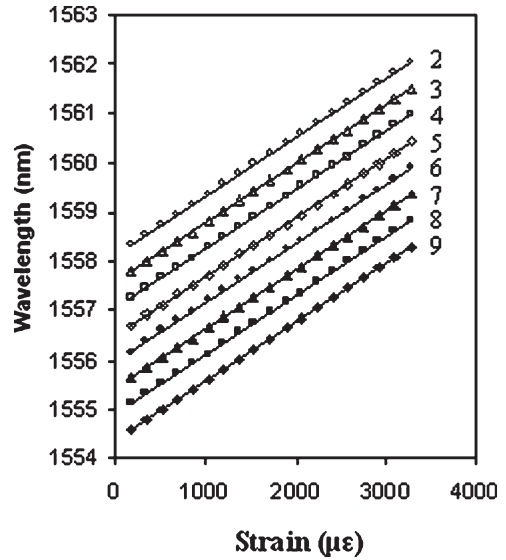

Fig. 3.   Strain dependence of the transmission wavelengths of the 2° slanted MFBG at room temperature. The strain sensitivities are 1.2034, 1.2026, 1.2018, 1.2005, 1.1989, 1.1971, 1.1962 and 1.1956 pm/$\mu\varepsilon$ for the second transmission dip up to the ninth transmission dip, respectively.
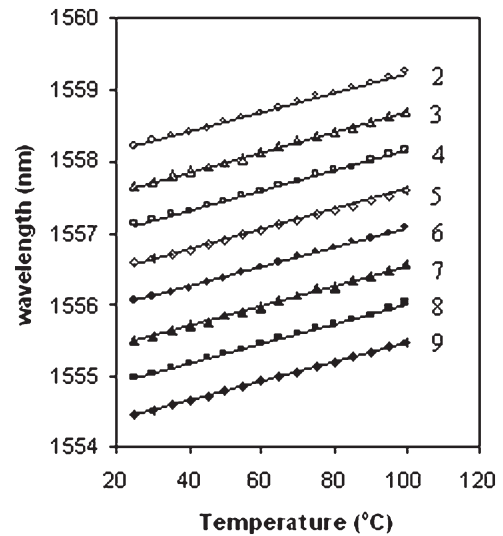

Fig. 4.   Temperature dependence of the transmission wavelength of the 2° slanted MFBG without strain. The temperature sensitivities are 13.831, 13.829, 13.825, 13.822, 13.819, 13.815, 13.811, and 13.806 pm/°C for the second transmission dip up to the ninth transmission dip, respectively.

of different transmission dips (from the second to the ninth) to be 1.2246, 1.2244, 1.2242, 1.2240, 1.2238, 1.2236, 1.2234 and 1.2231 pm/$\mu\varepsilon$, respectively. In addition, the temperature sensitivities are expected, from theory, to be 13.817, 13.813, 13.804, 13.800, 13.795, 13.791, and 13.787 pm/°C, respectively. Our experimental results are in good agreement with the theoretical predictions.
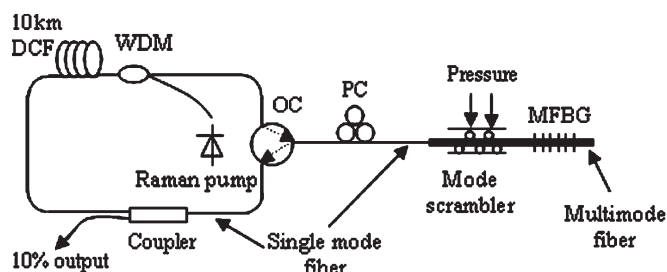
Fig. 5. Experimental setup of the multiwavelength Raman fiber laser. Thin line: SMF. Thick line: MMF.

IV. USING THE 2° SLANTED MFBG TO DEMONSTRATE A SWITCHABLE AND TUNABLE MULTIWAVELENGTH FIBER RAMAN RING LASER

Fig. 5 shows the configuration of the multiwavelength fiber Raman ring laser. The fiber that supplies the gain to the backward-pumped distributed Raman amplifier is a 10-km-long dispersion compensation fiber (DCF). The Raman pump module in Fig. 5 is formed by two wavelength- and polarization-multiplexed lasers whose wavelengths are 1425 and 1453 nm, respectively. We optimize the pump power ratios (300 and 500 mW) to obtain flat output signal power across the C-band. The optical circulator (OC) connects the slanted MFBG to the laser cavity and ensures that the light propagates in a single direction. The selected wavelength components reflected by the slanted MFBG propagate in the ring cavity. To get multiwavelength reflection peaks from the slanted MFBG, an MS is inserted to excite more modes. Meanwhile, a fiber coil polarization controller (PC) is inserted to adjust the polarization states of the different modes in the cavity. The laser output emerges from the 10% port of an optical coupler. The spectral characteristics of the laser are measured using the optical spectrum analyzer with a resolution of 0.02 nm.

The key components of the switchable multiwavelength Raman fiber laser are the MS and the slanted MFBG. The MS is used to adjust the mode excitation condition. When an SMF is spliced directly to an MMF that contains an MS with no pressure applied on it, this is the few-mode excitation condition that consists of only the fundamental mode and a few other higher order modes at a much reduced intensity. Applying pressure on the MS gives rise to the multimode excitation condition such that many modes are excited with large intensities. The state of multimode excitation can be changed by pressing on the surface of the MS with different pressures. One important property of the slanted MFBG is that the reflection of the slanted MFBG will change with changing mode excitation conditions, as shown in Fig. 6. Obviously, the reflection peaks of the slanted MFBG appear at the same wavelengths as the transmission dips. Curve 1 in Fig. 6 indicates that without the pressure on the MS, the mode couplings in the MFBG mainly occur from the forward zeroth to the backward zeroth principle mode. In addition, the couplings from the forward zeroth to the backward second, fourth, and sixth modes also appear with relatively low reflection intensity. This phenomenon is based on the fact that the modes with central symmetry are easier to guide than other kinds of modes when an SMF, which is a central symmetrical waveguide, is spliced directly to an MMF, which is another
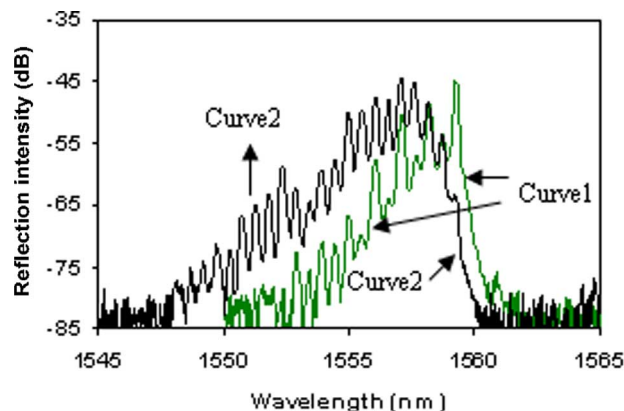

Fig. 6. Reflection spectra of the slanted MFBG under different mode excitation conditions. Curve 1: No pressure applied on the MS. Curve 2: Pressure applied on the MS. (Color version available online at http://ieeexplore.ieee.org.)

central symmetrical waveguide, with no pressure on the MS. When changing the mode excitation condition (i.e., changing the pressure on the MS), the wavelengths of the reflection peaks keep their original position, but the intensity of the reflection peaks shows a very large change as shown by curve 2 in Fig. 6. The reflection peaks increase in number when further pressure is applied on the MS because the number of the coupled modes increases. The multiwavelength laser's oscillating modes will correspond to the wavelengths of the high reflection intensities of the slanted MFBG; hence, the number and wavelength range of the laser modes will change according to mode excitation conditions.

By appropriately adjusting the pressure on the MS, the ring cavity laser can be made to operate in the single-, dual-, and multiwavelength states. The maximum number of wavelengths obtained is five. Fig. 7 represents some typical examples. Fig. 7(a) shows that only one lasing line occurs at 1557.63 nm. The full-width at half-maximum (FWHM) lasing linewidth is approximately 0.05 nm, and the side-mode suppression ratio (SMSR) is approximately 41 dB. The two lasing lines in Fig. 7(b) are at 1558.20 and 1558.73 nm, and the separation between the two lasing wavelengths is 0.53 nm. Dual wavelengths are excited at two adjacent reflection peaks. Fig. 7(c) shows four lasing lines at 1556.02, 1556.54, 1557.08, and 1557.63 nm. Fig. 7(d) shows five lasing lines at 1556.56, 1557.10, 1557.63, 1558.18, and 1558.71 nm with wavelength separation of approximately 0.54 nm. The linewidth of each oscillation is approximately 0.08 nm, and the SMSR is larger than 32 dB. The principle of wavelength switching is to balance the net gain (reflection intensity) at different reflection wavelengths of the slanted MFBG by adjusting the mode excitation condition. In the single-wavelength laser case, lasing is at the wavelength with the largest net gain. On the other hand, the laser will oscillate at multiple wavelengths simultaneously when the gains at those wavelengths are nearly the same. In the experiment, we find that the effect of the state of the PC is very small because the Raman amplifier has a very long gain fiber (10 km) as compared to an erbium-doped fiber amplifier (EDFA) or a SOA [11], [13]. The repeatability of the multiwavelength fiber Raman laser is good. The same set of wavelengths can lase repeatedly by applying the same pressure on the MS (while
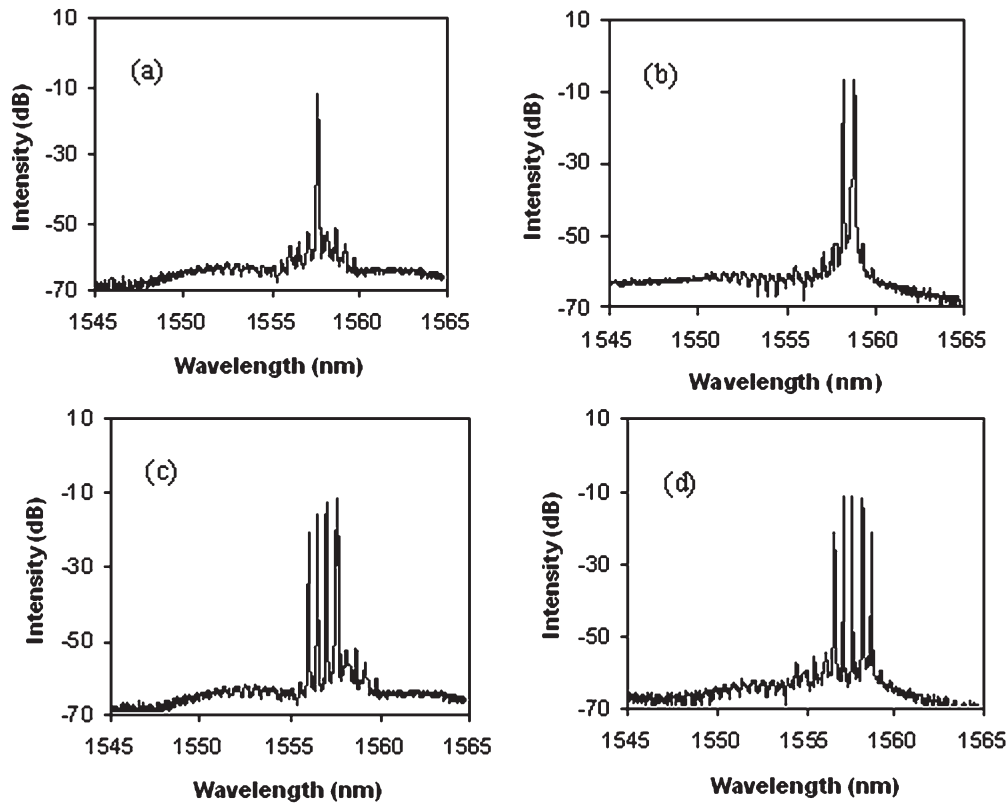
Fig. 7.   Spectra of the Raman fiber laser under different states of the MS.

keeping the other parameters unchanged). The wavelength stability and output power stability are also important characteristics of a laser. By monitoring the laser spectrum over a long time (∼ 2 h), we have observed that the ring cavity laser can operate stably under laboratory conditions. As an example, in a five-wavelength oscillation state, the wavelengths remain stable, and there are only slight power fluctuations. The extent of the fluctuation is approximately 0.5 dB. The stable operation of our multiwavelength fiber Raman laser is due to the following factors: 1) Raman gain is inhomogeneous, and therefore, mode competition [13] occurring in multiwavelength lasers can be effectively suppressed, and stable multiwavelength oscillation is supported. 2) The reflection peaks of the MFBG are not affected by random vibrations that are small in magnitude. 3) The mode excitation condition of the light excited by the MS is stable when the MS is fixed, and thus, the reflectivity of the MFBG at different reflection peaks remains unchanged. All of these reasons ensure that the multiwavelength fiber Raman ring laser has a good stability.

Furthermore, continuous wavelength tuning of the multi-wavelength fiber Raman ring laser is realized by axially straining the slanted MFBG. The wavelength-tuning range is limited by the amount of axial strain the MFBG can withstand. In our experiment, a 4.2-nm tuning range is obtained when a strain between 0 and 3612 $\mu\varepsilon$ is applied on the slanted MFBG. Fig. 8 shows the spectra of the dual-wavelength fiber Raman laser with different strain on the slanted MFBG. When the strain applied on the slanted MFBG is 1675 $\mu\varepsilon$, dual wavelengths become 2 nm longer as compared to the no-strain case. In addition, when the strain increases to 2656 $\mu\varepsilon$, the wavelengths shift
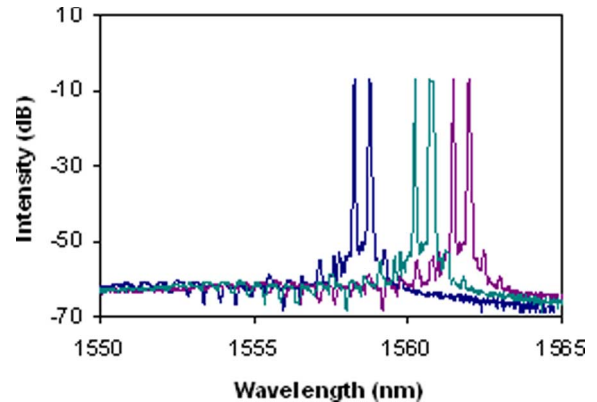

Fig. 8.   Tuning the wavelengths of the dual-wavelength fiber Raman laser by straining the 2° slanted MFBG with 0, 1675, and 2656 $\mu\varepsilon$ (from left to right), respectively. The pressure applied to the MS is the same in all three cases. (Color version available online at http://ieeexplore.ieee.org.)

by 3.2 nm. The shape of the laser output spectrum remains unchanged when only straining the slanted MFBG and fixing the MS and the PC. The wavelength separations between the excited wavelengths remain constant during the wavelength tuning because the strain sensitivities for the different resonant wavelengths of the slanted MFBG are almost uniform as reported in Section III. This property is very important for some applications. Moreover, the wavelength-tuning technique based on straining the MFBG is reliable. When the slanted MFBG is glued very well on the surfaces of the mover B and the fixed body A as shown in Fig. 2 and the axial strain applied on the MFBG is below the value that the MFBG can withstand,

the wavelength shift of the multiwavelength laser is linearly proportional to the strain, and the wavelength-tuning coefficient of the laser is the same as K_ε (~ 1.2 pm/$\mu\varepsilon$). When a certain axial strain is applied on the MFBG, the wavelength shift of the laser is also definite. As soon as a strain is not applied on the MFBG, the wavelengths of the multiwavelength laser will return to the original oscillation at once (that is, the MFBG is back to the free state). This also shows that the straining technique has a good repeatability, and it does not give rise to any hysteresis phenomenon.

The Raman ring laser configuration described in this section for realizing a switchable and tunable multiwavelength laser has the advantages of having a more stable operation and a simpler configuration compared with many other techniques. As is known, several FBGs with different single reflection wavelengths must be used in all kinds of multiwavelength fiber lasers by utilizing cascaded FBGs or complex topology FBGs written in SMFs. This increases the fabrication complexity and cost because every FBG needs a phase mask with a certain and carefully controlled Bragg period. At the same time, special FBGs such as sampled FBGs and overlap-written FBGs used in some configurations of multiwavelength fiber lasers need complex fabrication procedures and control software. On the other hand, the fabrication of an MFBG is as easy as that of an FBG written in an SMF. The MFBG is obtained using only one phase mask with a constant period. Those advantages are certified by our experimental results.

V. Conclusion

We have investigated the strain and temperature characteristics of a 2° slanted MFBG both theoretically and experimentally. Results show that the strain and temperature sensitivities are almost the same for different transmission dips of the 2° slanted MFBG. Furthermore, we have demonstrated a novel and simple multiwavelength fiber Raman ring laser by using the 2° slanted MFBG as a multireflection filter. Utilizing two characteristics of the 2° slanted MFBG, namely 1) resonant wavelength intensities strongly affected by excited mode propagating before the grating and 2) uniform strain sensitivities of different resonant wavelengths, wavelength switching, and continuous wavelength tuning are realized in the multiwavelength fiber Raman ring laser, respectively. Our results show that the laser can generate single-, dual-, three-, four-, and five-wavelength lasing by switching between each operation if we adjust an MS that is inserted in front of the slanted MFBG; furthermore, a 4.2-nm continuous wavelength-tuning range is achieved by straining the slanted MFBG when the MS is fixed. Such a laser has the advantages of having a more stable operation and a simpler configuration compared with other types of multiwavelength lasers that can be wavelength switched and wavelength tuned.

References

[1] G. Meltz, W. W. Morey, and W. H. Glenn, "Formation of Bragg gratings in optical fibers by a transverse holographic method," *Opt. Lett.*, vol. 14, no. 15, pp. 823–825, Aug. 1989.

[2] K. H. Wanser, K. F. Voss, and A. D. Kersey, "Novel fiber devices and sensors based on multimode fiber Bragg gratings," *Proc. SPIE*, vol. 2360, pp. 256–268, 1994.

[3] T. Mizunami, S. Gupta, T. Yamao, and T. Shimomura, "Multimode fiber Bragg gratings—Spectral characteristics and applications," in *Proc. Int. Conf. Integr. Opt. Opt. Fiber Commun./Eur. Conf. Opt. Commun.*, Sep. 1997, vol. 3, pp. 182–185.

[4] T. Mizunami, T. V. Djambova, T. Niiho, and S. Gupta, "Bragg gratings in multimode and few-mode optical fibers," *J. Lightw. Technol.*, vol. 18, no. 2, pp. 230–235, Feb. 2000.

[5] T. Szkopek, V. Pasupathy, J. E. Sipe, and P. W. E. Smith, "Novel multimode fiber for narrow-band Bragg gratings," *IEEE J. Sel. Topics Quantum Electron.*, vol. 7, no. 3, pp. 425–433, May/Jun. 2001.

[6] T. Mizunami, T. Niiho, and T. V. Djambova, "Multimode fiber Bragg gratings for fiber bending sensors," *Proc. SPIE*, vol. 3746, pp. 216–219, 1999.

[7] X. Feng, Y. Liu, S. Fu, S. Yuan, and X. Dong, "Switchable dual-wavelength ytterbium-doped fiber laser based on a few-mode fiber grating," *IEEE Photon. Technol. Lett.*, vol. 16, no. 3, pp. 762–764, Mar. 2004.

[8] L. Su, C. Lu, J. Hao, Z. Li, and Y. Wang, "Design of wavelength-switching erbium-doped fiber lasers with a multimode Bragg grating using spatial-mode excitation and selection techniques," *IEEE Photon. Technol. Lett.*, vol. 17, no. 2, pp. 315–317, Feb. 2005.

[9] H.-G. Yu, Y. Wang, C.-Q. Xu, and A. D. Vandermeer, "Oscillation wavelength selection of semiconductor lasers using a multimode fiber Bragg grating," *Opt. Express*, vol. 13, no. 5, pp. 1660–1665, Mar. 2005.

[10] X. Yang, C. Zhao, J. Zhou, J. Guo, X. Ng, X. Zhou, and C. Lu, "The characteristics of fiber slanted gratings in multimode fiber," *Opt. Commun.*, vol. 229, no. 1–6, pp. 161–165, Jan. 2004.

[11] C.-L. Zhao, Z. Li, M. S. Demokan, X. Yang, and W. Jin, "Switchable multiwavelength SOA-fiber ring laser based on a slanted multimode fiber Bragg grating," *Opt. Commun.*, vol. 252, no. 1–3, pp. 52–57, 2005.

[12] A. Othonos and K. Kalli, *Fiber Bragg Gratings—Fundamentals and Applications in Telecommunications and Sensing*. London, U.K.: Artech House, 1999.

[13] C.-L. Zhao, X. Yang, C. Lu, J. Ng, X. Guo, P. R. Chaudhuri, and X. Dong, "Switchable multi-wavelength erbium-doped fiber lasers by using cascaded fiber Bragg gratings written in high birefringence fiber," *Opt. Commun.*, vol. 230, no. 4–6, pp. 313–317, Feb. 2004.

Chun-Liu Zhao received the B.S. degree in applied physics from Inner Mongolia University, Huhehaote, China, and the M.S. and Ph.D. degrees in optics from Nankai University, Tianjin, China, in 1999 and 2002, respectively.

From 2002 to 2004, she was a Research Fellow with the Lightwave Department, Institute for Infocomm Research, Singapore. Since 2004, she has been working as a Postdoctoral Fellow in the Department of Electrical Engineering, Hong Kong Polytechnic University, Kowloon, Hong Kong. Her research interests include fiber grating, optical fiber amplifiers and lasers, and applications based on photonic-crystal fibers.

Zhaohui Li was born in Inner Mongolia, China. He received the B.S. degree from the Department of Physics and the M.S. degree from the Institute of Modern Optics, Nankai University, Tianjin, China. He is currently working toward the Ph.D. degree at the Nanyang Technological University, Singapore.

His research interests include Raman amplifiers, transmission systems, and optical access networks.

M. S. Demokan (SM'89) received the B.Sc. degree from the Middle East Technical University, Ankara, Turkey, in 1970 and the M.Sc. and Ph.D. degrees from King's College, University of London, London, U.K., in 1972 and 1976, respectively, all in electronic engineering.

He served in the Middle East Technical University in various capacities including Dean of Faculty, Head of Department, and Associate Professor between 1976 and 1983. After conducting research for a year at Imperial College, University of London, as a Visiting Senior Research Fellow, he joined the Hirst Research Center, General Electric Company, U.K., in 1984, where he directed contract research as the Head of the Department of Optoelectronic Components and as the Chief Scientist of the Department of Optical Communications. Since 1988, he has been with the Hong Kong Polytechnic University, Kowloon, Hong Kong, where he was promoted to Chair Professor in 1992. He was the Head of the Department of Electrical Engineering between 1988 and 1995, the Dean of the Faculty of Engineering between 1995 and 2000, an Associate Vice President between 1997 and 2000, and the Vice President overseeing university research and academic appointments and promotion between 2000 and 2003. He has been the Vice President responsible for academic development since 2005. He published two books and more than 180 refereed papers, served on the Editorial Board of two international journals, organized various international conferences, and served in various capacities in professional bodies. His current research interests include optical communication systems (especially all-optical switching and photonic-crystal fibers) and various types of optical sensors.

Prof. Demokan is a Fellow of the Hong Kong Institution of Engineers and the Institution of Electrical Engineers (U.K.).

Xiufeng Yang received the M.E. degree in communication from Tianjin University, Tianjin, China, in 1994 and the Ph.D. degree in optics from Nankai University, Tianjin, in 1998.

She is currently a Research Scientist in the Institute for Infocomm Research, Singapore. She is active in the field of fiber optical strain sensor, temperature sensor, interrogation system, and erbium-doped fiber lasers and amplifiers.

Wei Jin (M'95–SM'98) received the B.Eng. and M.Sc. degrees from the Beijing University of Aeronautics and Astronautics, Beijing, China, in 1984 and 1987, respectively, and the Ph.D. degree in fiber optics from the University of Strathclyde, Glasgow, U.K., in 1991.

From 1991 to 1995, he was a Postdoctoral Research Fellow at the University of Strathclyde. He joined the Department of Electrical Engineering, Hong Kong Polytechnic University, Kowloon, Hong Kong, in 1996 and is currently a Full Professor. He authored or coauthored two books, over 300 journals and conference publications, and five patents, all in the area of fiber optic devices and sensors.

Prof. Jin received the President Award of the Hong Kong Polytechnic University for outstanding performance in research and scholarly activities. He secured research funds of over HK\$25 million over the past several years. He is a member of SPIE and OSA.

Chao Lu (M'91) received the B.Eng. degree from Tsinghua University, Beijing, China, in 1985 and the M.Sc. and Ph.D. degrees from the University of Manchester, Manchester, U.K., in 1987 and 1990, respectively.

In 1991, he joined the Nanyang Technological University, Singapore, where he is currently an Associate Professor. Since 2002, he has also been with the Institute for Infocomm Research, Singapore, where he has been leading a group of researchers working in the areas of fiber devices, high-capacity optical transmission systems, and optical access network test beds.